Zeitschrift für Kristallographie 201, 263–281 (1992)
© by R. Oldenbourg Verlag, München 1992 – 0044-2968/92 $3.00+0.00

Beraunite: Refinement, comparative crystal chemistry, and selected bond valences

Paul B. Moore and Anthony R. Kampf*

The Department of the Geophysical Sciences, The University of Chicago, Chicago, Illinois 60637 USA

Received: July 12, 1991

Beraunite / Phosphate / Fe(II)–Fe(III) / Hydroxy-oxy / Octahedral face-sharing / Cation repulsion / Antitypy (partial)

Abstract. Deep green beraunite from Campanian age marls of Mullica Hill, N. J. (USA) was investigated owing to its unique crytal chemistry (two previous refinements involved orange crystals). Our crystal gave nearly $4[Fe^{2+}Fe_5^{3+}(OH)_5(H_2O)_4(PO_4)_4 \cdot 2H_2O]$, $a = 20.953(5)$, $b = 5.171(1)$, $c = 19.266(4)$ Å, $\beta = 93.34(2)°$, $C2/c$, $R = 0.043$ (isotropic) for 2065 unique F_o and 91 variable parameters.

Common to several known "ferrosoferric" phosphate structures, the underlying principle is a linear face-sharing oxygen octahedral trimer whose cations are M(4)–M(1)–M(4). For our beraunite, ca. 83% Fe^{2+} resides in the central M(1) site with mean M(1)–O = 2.11 Å. The other octahedral cation sites M(2), M(3), and M(4) (mean M–O distances 2.01 to 2.02 Å) are Fe^{3+}. The orange crystals of the other studies have predominant Fe^{3+} at all M(1) to M(4) octahedral sites (mean M–O distances 1.97 to 2.04 Å). Distortion of the octahedral face-trimer is pronounced, with M(1)–M(4) distance lengthening of 19% compared with the perfect octahedral model. This results from cation-cation repulsion, which distorts the entire immediate environment from the perfect model.

The OH(1) site on the trimer is coordinated by M(1), M(3), M(4), and H(1). Bond valence computations for the trimer suggest that $Fe^{2+}Fe^{3+}$ (green) → $Fe^{3+}Fe^{3+}$ (orange) may involve (1) O–H(1) distance response to bond valence deviation or (2) an averaged model $2OH^- \rightarrow 2(OH_{1/2}O_{1/2})^{1.5-}$, but independent spectroscopic study is required to unravel the mechanism.

* *Present address:* Natural History Museum of Los Angeles County, 900 Exposition Blvd., Los Angeles, California 90007 USA.

The aristotype for this family of structures is believed to be "ideal" lipscombite, $Fe_8^{2+}(OH)_4(PO_4)_4$, $I4_1/amd$. Included are the several 5×14 Å^2 derivatives; scheelite, $CaWO_4$, which shares partial antitypy; and MHSH = $(Mg_{16/3}\square_{8/3})(OH)_4(SO_4)_4(H_{4/3})$, $I4_1/amd$ with similar cell metric.

Introduction

Beraunite, ferrous end-member $Fe^{2+}Fe_5^{3+}(OH)_5(H_2O)_4(PO_4)_4 \cdot 2H_2O$, is one of a rather significant family of mineral species whose crystal structures are based on a particular fundamental building block: the linear $Fe^{3+} - Fe^{2+,3+} - Fe^{3+}$ oxygen octahedral face-sharing trimer. Variously called the "5 Å fiber axis structures" (the fiber direction is parallel to an octahedral plus a tetrahedral edge) or the "ferrosoferric phosphates" (both Fe^{2+} and Fe^{3+} occur in the structure), the phases range from greenish-black color for $Fe^{2+} - Fe^{3+}$ compositions to orange, tan and yellow hues for the oxidized $Fe^{3+} - Fe^{3+}$ compositions. They occur associated with "bog iron ores" in siliceous sediments and novaculites, as secondary hydrothermally reworked products of primary transition metal phosphates in pegmatites, and as replacements of bones and shells in Mesozoic and Cenozoic marls. The linear $Fe^{3+} - Fe^{2+,3+} - Fe^{3+}$ oxygen octahedral face-sharing trimer has been established by varying degrees of refinement in phases such as rockbridgeite, beraunite, dufrenite, barbosalite and more than one ordered type of lipscombite. The phases above are arranged in approximate order of decreasing natural abundance. Several other phases such as kidwellite and laubmannite have been inferred by physical characters, XRD, and paragenesis to belong to this same group. Moore (1970) offered the first chemical crystallographic discussion on these perplexing phases.

The first crystal structure analysis and refinement ($R = 0.066$) of an oxidized reddish-brown beraunite was presented by Fanfani and Zanazzi (1967). We refined a reduced deep greenish-black crystal about 15 years ago, and the results are reported in the present study. A manganese-bearing red beraunite was studied ($R = 0.034$) and recently reported by Marzoni Fecia di Cossato, Orlandi and Pasero (1989). The first structure investigation of a synthetic tetragonal lipscombite (called "iron lazulite") was reported by Katz and Lipscomb (1951). This approximate determination was not refined in the conventional contemporary sense, but the study appears to be a careful investigation and leads to approximately $Fe_7^{2.29+}(OH)_4(PO_4)_4$ for a crystal shown to be partially disordered. We consider it justified to quote the structure results because its space group $I4_12_12$ is a nearest subgroup of parent $I4_1/amd$. Recently, another synthetic lipscombite with $a' = \sqrt{2}\,a$ of Katz and Lipscomb, space group $P4_32_12$ (a subgroup of $I4_32_12 \equiv I4_12_12$) has been reported by Vencato, Mattievich and Mascarenhas (1989). This crystal, too, is disordered, $R = 0.102$, cell

contents *ca.* $4Fe^{2+}Fe_2^{3+}(OH)_2(PO_4)_2$. The cell contents of the primitive group can be related to that of the body-centered lipscombite. While the Fe atoms in the octahedral site are evidently disordered with vacancies in the body-centered phase, three unique Fe positions occur in the primitive phase, a consequence of ordered vacancies over the stacks of $\overset{1}{\infty}$ $Fe^{2+}\phi_3$ (ϕ = generalized anion) octahedral face-sharing chains. Finally, a remarkable phase, seemingly totally unrelated to lipscombite, is included. It is $Mg SO_4 \cdot 1/3 Mg(OH)_2 \cdot 1/3 H_2O$, with cell contents $(\square_{8/3}Mg_{16/3})(\square_{32/3}H_{16/3})$-$(SO_4)_4$, space group $I4_1/amd$, $R = 0.041$ reported by Keefer, Hochella Jr. and De Jong (1981). For brevity, the phase is called MHSH. We shall also employ other acronyms for brevity, in particular MK for this study, MOP for Marzoni Fecia de Cossato et al. (1989), and FZ for Fanfani and Zanazzi (1967). These constitute the three structure studies on beraunite. Compared with the other ferrosoferric phosphate structure types, beraunite is the most open and the $Fe^{3+} - Fe^{2+,3+} - Fe^{3+}$ trimers, although bridged, are well-separated.

The distribution of Fe^{2+} in the beraunite structure has remained enigmatic. Does it occur at the center of the trimer? Is it at the periphery of the trimer? Is it disordered and distributed over various unique Fe sites? These questions we sought to answer by means of chemical crystallography.

Experimental

For a rather complex crystal structure with four independent Fe sites and with little material at hand, a Mössbauer resonance experiment was ruled out. Rather, an X-ray diffraction experiment was considered appropriate, the results of which would employ chemical analysis, bond distances and bond angles as an analytical tool. By good fortune, we received an unusual specimen over 15 years ago of an uncommon green-black platy mineral from Mullica hill, Gloucester Co., New Jersey, USA. It consisted of belemnite fragments in marl of Campanian age with interstices containing the green-black mineral (which proved to be beraunite), blue blades of vivianite and scattered mats of ferrostrunzite. We garnered as much material as available toward oxidation grade determination and eventual crystal structure analysis. A few plates large enough for structure study were examined by single crystal Buerger precession film camera and MoK_α radiation. From several fragments, one particularly suitable crystal was selected.

Oxidation grade

Very little uncontaminated Mullica Hill beraunite could be obtained. Promising aggregates were coarsely crushed in acetone, the pure deep-green plates separated by needle. Two batches were separated: about 20 mg for

Table 1. Oxidation grade of Mullica Hill beraunite (wt.%).

	[1]	[2]	[3]	[4]	[5]	[6]
FeO	7.91	47.47	46.3(5)	14.8(5)	1.92	–
Fe_2O_3	43.97	–	–	–	54.41	52.81
P_2O_5	31.26	–	–	–	30.17	31.30
H_2O	16.86	–	–	–	13.45	15.89
Total	100.00	–	–	–	99.97	100.00

Notes: [1] Beraunite, $Fe^{2+}Fe_5^{3+}(OH)_5(H_2O)_4(PO_4)_4 \cdot 2H_2O$; [2] beraunite, all Fe as FeO; [3] Mullica Hill beraunite, total Fe as FeO (AAS), no Al detected, J. Ito, analyst; [4] Mullica Hill sample wt. 9.9 mg, $KMnO_4$ titration, J. Ito, analyst; [5] Hallowell analysis of Middletown, N. J. beraunite, incl. 0.02% Al_2O_3 (Frondel, 1949); [6] "oxy-beraunite", $Fe_6^{3+}O(OH)_4(H_2O)_4(PO_4)_4 \cdot 2H_2O$.

total iron by atomic absorption spectrophotometry. The other batch, about 10 mg, was put toward oxidation grade determination by $KMnO_4$ titration. The late Dr. Jun Ito performed all the analyses in 1976.

The results, compared with end-members and an earlier published brownish sample from Middletown, NJ, USA, appear in Table 1. It is seen that total iron reported as FeO approximates the theoretical value, but the determination of FeO content in our sample is high by a factor of 1.87 compared with the theoretical reduced beraunite. On structural grounds, further reduction of iron in the crystal is not likely. The answer to this discrepancy was soon found in optically and X-ray examined platy beraunites: they included flecks and patches of thin vivianite which seemed to have partially replaced beraunite at some later event. Vivianite, $Fe_3^{2+}(H_2O)_8(PO_4)_2$, would easily provide excess FeO determined in the earlier analysis by Dr. Ito. Eventual crystal structure analysis gave an estimate of *ca.* 83% Fe^{2+} in the M(1) or "reduced" site. This corresponds to about 6.6 wt % FeO in our samples, and means that the beraunite sample analyzed for FeO is constituted of about 20% vivianite formula. A simple valence balance calculation can be made as an independent check. Taking reduced beraunite and vivianite as end-members and normalizing to the same oxygen content, the amount of admixed vivianite is about 14.5%, again indicating some vivianite contaminent in the chemical analysis.

Experimental structural crystallography of Mullica Hill beraunite

This study was completed over 12 years ago, was resurrected when the remarkable relationship to lipscombite was discovered, and when a recent independent beraunite refinement was reported. The lapse in time should be borne in mind when appraising the procedures used in the present study.

Coarse crystals of deep green beraunite were selected, and gently broken under acetone. The pieces measuring 100—1000 μm were examined under a binocular microscope and, from several selections, a brilliant uniform flake was chosen. It was a rectangular plate, measuring $200(\|a) \times 420(\|b) \times 600(\|c)$ μm^3, bounded by six faces. It proved to be an excellent crystal from several precession photographs of $(h0l)$, $(h1l)$, and $(hk0)$ projections using MoK_α radiation. This relatively large crystal was deemed ideally suitable for crystal structure analysis. For $4[Fe^{2+}Fe_5^{3+}(OH)_5(H_2O)_4(PO_4)_4 \cdot 2H_2O]$, we calculated $\mu_l = 47.7$ cm^{-1} for MoK_α radiation. The crystal was mounted on a PICKER FACS-1 automated diffractometer. Least squares refinement of 30 reflections between $20° < 2\theta < 40°$ gave $a = 20.953(5)$, $b = 5.171(1)$, $c = 19.266(4)$ Å, $\beta = 93.34(2)°$, space group $C2/c$ or Cc.

From the ideal end-member formula, the cell contents and cell volume give a computed density D(calc) = 2.894(1) g cm^{-3}, within the range D(obs) = 2.8—2.99 reported in Palache, Berman, and Frondel (1951). Single crystal data were collected to $2\theta = 50°$ with graphite monochromatized MoK_α radiation, scan speed 2° min^{-1}, 20 s stationary background counts on each side of the peak, half-angle scan width 1.0°—3.0°, increasing for higher angles. The data were processed including anomalous dispersion correction, f'' [Cromer and Liberman (1970)] and absorption correction using the methods of Gaussian integration (Burnham, 1966). These afforded the $|F_o|$ employed in ensuing refinement.

No secondary extinction correction was performed on our crystal. Scattering factors for Fe^{3+}, P^{5+}, and O^{1-} refer to Cromer and Mann (1968). Isotropic displacement parameters were used throughout. We initiated our cycles with atomic coordinate and thermal parameters of Fanfani and Zanazzi (1967) for their well-refined orange beraunite.

After five cycles, all parameter shifts were within their limits of error at $R = 0.05$, whereupon a difference Fourier synthesis was requested. The end-member formula required that nine independent H-atoms occur in the asymmetric unit. Each H-atom is labelled according to its donor: HO(n) for the n-th H-atom attached to hydroxyl oxygen OH(n) and HW(ma) and HW(mb) for the two H-atoms bonded to the m-th water oxygen, W(m). Of the expected nine independent H-atoms, only six could be unambiguously located. These were refined in the subsequent cycles. Another difference Fourier synthesis failed to provede additional peaks beyond a high noise level. The centroids for HO(3), HW(1b), and HW(3b) were computed from inferred bond distances and angles and therefore are mere approximations. At the final cycle, $R = 0.043$ and $R_w = 0.035$ for 2065 unique reflections above $2\sigma|F_o|$, where $R = \Sigma\|F_o|-|F_c\|/\Sigma|F_o|$ and $R_w = [\Sigma_w\|F_o|-|F_c\|^2/\Sigma_w|F_o|^2]^{1/2}$ where $w = \sigma^{-2}$ of $|F_o|$.

For isotropic displacement parameter refinement, the low R-index suggests a good data set and, if contemporary refinement were initiated,

Table 2. Mullica Hill beraunite: atomic coordinate parameters.

Atom	x	y	z	B(Å^2)
M(1)	0	0	0	0.73(2)
M(2)	1/4	1/4	0	0.68(2)
M(3)	0.04430(3)	0.2847(1)	0.17278(4)	0.62(1)
M(4)	0.10813(3)	0.0389(1)	0.41529(4)	0.64(1)
P(1)	0.10518(6)	0.4743(2)	0.02374(6)	0.51(2)
O(1)	0.1779(2)	0.4837(6)	0.0161(2)	0.74(6)
O(2)	0.4245(2)	0.2515(6)	0.0199(2)	0.76(6)
O(3)	0.4234(2)	0.2327(6)	0.5039(2)	0.82(6)
O(4)	0.0906(2)	0.4418(7)	0.1000(2)	1.09(6)
P(2)	0.40726(6)	0.04656(2)	0.18157(6)	0.60(2)
O(5)	0.4788(2)	0.0525(6)	0.1667(2)	0.82(6)
O(6)	0.1004(2)	0.4930(6)	0.2404(2)	0.97(6)
O(7)	0.3783(2)	0.3136(6)	0.1638(2)	0.88(6)
O(8)	0.1294(2)	0.3431(6)	0.3626(2)	0.98(6)
OH(1)	0.0074(2)	0.0405(7)	0.3913(2)	0.78(6)
OH(2)	0.1926(2)	0.0219(7)	0.4620(2)	1.06(6)
OH(3)	0	0.1142(9)	1/4	0.90(8)
W(1)	0.3841(2)	0.4915(8)	0.3192(2)	1.89(7)
W(2)	0.2472(2)	0.0857(8)	0.0988(2)	1.38(7)
W(3)	0.2318(2)	0.3639(9)	0.2165(3)	3.10(10)
HO(1)	0.002(2)	0.89(1)	0.379(3)	0.8
HO(2)	0.194(3)	0.10(1)	0.481(3)	1.0
HO(3)	0	−0.10	1/4	n.a.
HW(1a)	0.386(3)	0.38(1)	0.313(3)	1.8
HW(1b)	0.379	0.50	0.291	n.a.
HW(2a)	0.243(3)	0.19(1)	0.134(3)	1.3
HW(2b)	0.286(3)	0.02(1)	0.108(3)	1.3
HW(3a)	0.206(3)	0.40(1)	0.211(3)	2.9
HW(3b)	0.230	0.29	0.225	n.a.

Notes: Standard errors for refined parameters refer to the last digit. Atoms are grouped: octahedral cations, phosphate tetrahedra, hydroxyls, water molecules, hydrogen atoms. Errors with no physical meaning are not stated. The n.a. refer to distance calculated parameters; they were not refined.

the anisotropic displacement mode would surely lead to much better convergence and the possibility of locating the three missing H-atoms. We earlier attempted anisotropic displacement parameter refinement, but two independent water molecules and one hydroxyl group converged to non-positive definite values, and therefore we decided to remain in isotropic mode. The independent $|F_o|$:variable parameter ratio is 2065:91 = 22.7.

Table 2 lists the atomic coordinate and displacement parameters and Table 2a [1] the $|F_o|-|F_c|$ tables. Table 3 lists the pertinent polyhedral bond distances and angles.

Chemical crystallography

The "iron lazulite"

Katz and Lipscomb (1951) investigated the crystal structure of synthetic "iron lazulite" in considerable detail. The shiny, jewel-like black crystals were prepared by Prof. J. W. Gruner (University of Minnesota) from a mix of $FePO_4$, FeO(OH) and H_2O heated to 170° C at about 28 bars pressure. Specific gravity in Clerici solution gave D(obs) = 3.8. Complete chemical analysis was not possible, but Prof. Gruner reported phosphate as the most important anion present.

Katz and Lipscomb studied a single crystal of pseudo-octahedral shape and showed it to be uniquely $I4_122$ ($\equiv I4_12_12$, etc.), an immediate subgroup of holosymmetric $I4_1/amd$. In fact, they note that of some 150 unique reflections on Weissenberg films, only three weak (110), (310), and (114) reflections violated the holosymmetric group. This was later shown to be due to the distortion of (PO_4) tetrahedra away from $\{\bar{4}2m = T_d\}$ symmetry. Furthermore, they showed that the calculated molecular weight, based on the determined specific gravity and unit cell volume, violated completely occupied atom sites. Such sites, already established from structure analysis, would have required $Fe_8(OH)_4(PO_4)_4$ in the cell. A one-eighth average vacancy over the Fe positions was suggested, that is $Fe_7(OH)_4(PO_4)_4$. Our calculation from their data, assuming fully occupied anions gives $Fe_{7.12}$ in the cell. The average charge on the metal would lead to $Fe_{7.12}^{2.25+}(OH)_4(PO_4)_4$, or a $Fe^{2+}:Fe^{3+} = 3:1$ mixed-valence compound. A Pauling-type electrostatic valence balance of cations about anions presents excellent electrostatic neutrality about both the hydroxyl oxide and the phosphate oxide. Because the Katz and Lipscomb study did not report an *R*-index and because the atomic coordinates are only approximate, a refinement is highly desirable, and subtle problems in order-disorder, space group definition and displacement anisotropy are anticipated. Their proposed coordinates are adequate for our needs. The structure is represented as polyhedral diagrams in Figure 1a and Figure 1b.

To relate the "iron lazulite" or lipscombite structure type (which hereafter will be adopted as the *aristotype* of the 5×14 Å^2 structures: a host of other structure types including beraunite, dufrenite, rockbridgeite, etc., see Moore, 1970), it is convenient to explore the $I4_1/amd$ supergroup which

[1] Additional material to this paper can be ordered from the Fachinformationszentrum Karlsruhe, D-7514 Eggenstein-Leopoldshafen 2, Federal Republic of Germany. Please quote reference no. CSD 55710, the names of the authors and the title of the paper.

Table 3. Beraunite polyhedral distances and angles.

	M(1)				M(2)		
	MK	MOP	FZ		MK	MOP	FZ
$2M(1)-O(2)^{(4)}$	2.090	2.048	2.01	$2M(2)-OH(2)^{(3)}$	1.963	1.951	1.93
$2M(1)-OH(1)^{(2)}$	2.119	2.022	2.01	$2M(2)-O(1)$	1.973	1.975	1.94
$2M(1)-O(3)^{(6)}$	2.122	2.066	2.03	$2M(2)-W(2)$	2.089	2.070	2.04
average	2.110	2.045	2.02	average	2.008	1.999	1.97
	MK	$\phi-M-\phi'(^{\circ})$			MK		
$2O(2)^{(4)}-OH(1)^{(2)}$	2.629*	77.3		$2O(1)-OH(2)^{(3)}$	2.728	87.8	
$2O(2)^{(5)}-O(3)^{(6)}$	2.685*	79.2		$2O(1)-W(2)$	2.810	87.5	
$2O(3)^{(7)}-OH(1)^{(2)}$	2.686*	78.6		$2O(1)-OH(2)^{(6)}$	2.838	92.3	
$2O(2)^{(4)}-O(3)^{(6)}$	3.246	100.8		$2OH(2)^{(3)}-W(2)$	2.866	90.0	
$2O(3)^{(6)}-OH(1)^{(2)}$	3.283	101.4		$2OH(2)^{(6)}-W(2)$	2.868	90.0	
$2O(2)^{(5)}-OH(1)^{(2)}$	3.287	102.7		$2O(1)-W(2)^{(5)}$	2.935	92.5	
average	2.969	90.0		average	2.841	90.0	
	P(1)				P(2)		
	MK	MOP	FZ		MK	MOP	FZ
$P(1)-O(4)$	1.527	1.514	1.51	$P(2)-O(8)^{(6)}$	1.532	1.538	1.51
$P(1)-O(1)$	1.540	1.530	1.53	$P(2)-O(7)$	1.539	1.537	1.53
$P(1)-O(3)^{(6)}$	1.546	1.549	1.56	$P(2)-O(5)$	1.542	1.534	1.53
$P(1)-O(2)^{(5)}$	1.548	1.558	1.57	$P(2)-O(6)^{(6)}$	1.545	1.531	1.54
average	1.540	1.538	1.54	average	1.540	1.535	1.53
	MK				MK		
$O(1)-O(3)^{(6)}$	2.494	107.8		$O(7)-O(8)^{(6)}$	2.489	108.3	
$O(3)^{(6)}-O(4)$	2.507	109.3		$O(5)-O(7)$	2.500	108.4	
$O(2)^{(5)}-O(4)$	2.519	110.0		$O(6)^{(6)}-O(7)$	2.502	108.4	
$O(1)-O(4)$	2.520	110.5		$O(6)^{(6)}-O(8)^{(6)}$	2.519	109.9	
$O(2)^{(5)}-O(3)^{(6)}$	2.523	109.3		$O(5)-O(6)^{(6)}$	2.528	109.9	
$O(1)-O(2)^{(5)}$	2.529	109.9		$O(5)-O(8)^{(6)}$	2.546	111.8	
average	2.515	109.5		average	2.514	109.5	

contains $I4_122$ as one of its subgroups. The 4(*a*) and 4(*b*) Wyckoff positions for P and OH respectively remain invariant in both space groups and differ only in point symmetry. The 8(*f*) position for Fe corresponds to 8(*d*) in the holosymmetric group if a small movement to $x = \frac{1}{2}$ is tolerated. The same applies to 16(*g*), the general oxygen position for $I4_122$ "iron lazulite", which becomes 16(*h*) with $x \sim \frac{1}{4}$ and $y = 0$ for $I4_1/amd$. It is these small movements (<0.1 Å) for Fe and O atom positions which likely led to the

Table 3. (Continued).

	M(3)				M(4)		
	MK	MOP	FZ		MK	MOP	FZ
M(3)–O(4)	1.931	1.945	1.95	M(4)–O(8)	1.938	1.913	1.93
M(3)–O(5)$^{(4)}$	1.948	1.945	1.94	M(4)–OH(2)	1.941	1.933	1.93
M(3)–OH(3)	2.003	1.992	1.99	M(4)–O(7)$^{(6)}$	1.952	1.927	1.92
M(3)–O(6)	2.015	2.036	2.02	M(4)–O(2)$^{(6)}$	2.083	2.145	2.14
M(3)–OH(1)$^{(2)}$	2.034	2.011	1.99	M(4)–O(3)$^{(5)}$	2.092	2.194	2.20
M(3)–W(1)$^{(6)}$	2.133	2.121	2.12	M(4)–OH(1)	2.134	2.080	2.08
average	2.011	2.008	2.00	average	2.023	2.032	2.03

	MK			MK	
O(4)–O(6)	2.714	86.9	O(2)$^{(6)}$–OH(1)	2.629*	77.1
OH(1)$^{(2)}$–OH(3)	2.745	85.7	O(2)$^{(6)}$–O(3)$^{(5)}$	2.685*	80.0
O(4)–O(5)$^{(4)}$	2.797	92.3	O(3)$^{(5)}$–OH(1)	2.686*	78.9
O(5)$^{(4)}$–OH(3)	2.797	90.1	O(7)$^{(6)}$–O(8)	2.788	91.6
O(4)–W(1)$^{(6)}$	2.834	88.3	O(8)–OH(2)	2.808	92.8
O(5)$^{(4)}$–O(6)	2.860	92.3	O(3)$^{(5)}$–OH(2)	2.853	90.0
O(6)–W(1)$^{(6)}$	2.863	87.2	O(2)$^{(6)}$–OH(2)	2.864	90.7
OH(1)$^{(2)}$–W(1)$^{(6)}$	2.873	87.1	O(3)$^{(5)}$–O(8)	2.885	91.4
O(6)–OH(3)	2.888	91.9	O(7)$^{(6)}$–OH(1)	2.922	91.2
O(5)$^{(4)}$–OH(1)$^{(2)}$	2.895	93.2	O(7)$^{(6)}$–OH(2)	2.969	99.4
OH(3)–W(1)$^{(6)}$	2.908	89.3	O(2)$^{(6)}$–O(7)$^{(6)}$	3.007	96.3
O(4)–OH(1)$^{(2)}$	2.932	95.3	O(8)–OH(1)	3.075	97.9
average	2.842	90.0	average	2.848	89.8

H-bonds

HO(1)	OH(1)→O(5)$^{(6)}$	2.782(5)	HW(2a)	OW(2)→OW(3)	2.719(6)
HO(2)	OH(2)→O(1)$^{(3)}$	2.785(5)	HW(2b)	OW(2)→O(8)$^{(6)}$	2.931(5)
HO(3)	OH(3)→O(7)$^{(6)}$	3.346(6)			
			HW(3a)	OW(3)→O(6)	2.896(6)
HW(1a)	OW(1)→O(7)	3.128(5)	HW(3b)	OW(3)→OW(3)$^{(6)}$	2.970(6)
HW(1b)	OW(1)→O(6)$^{(6)}$	2.848(5)			

Notes: MK = this study ($\sigma = \pm 0.004$ Å), MOP = Marzoni Fecia di Cossato et al. (1989) ($\sigma = \pm 0.003$ Å), FZ = Fanfani and Zanazzi (1967) ($\sigma = \pm 0.01$ Å) for M–ϕ and P–O distances. The MK O–O′ edge distances are ± 0.005 Å, the angles $\pm 0.2°$. Referred to Table 2, the equivalences are designated as superscripts: (1) = $-x, -y, -z$; (2) = $-x, y, 1/2-z$; (3) = $x, -y, 1/2+z$; (4) = $1/2+x, 1/2+y, z$; (5) = $1/2-x, 1/2-y, -z$; (6) = $1/2-x, 1/2+y, 1/2-z$; (7) = $1/2+x, 1/2-y, 1/2+z$. Shared edges between octahedra, which in beraunite correspond to shared faces, are designated by asterisks (*).

three weak reflections noted by Katz and Lipscomb (1951) and forced $I4_122$ instead of holosymmetric $I4_1/amd$.

Unit cell and atomic coordinate parameters for the "iron lazulite" (hereafter referred to a lipscombite) studied by Katz and Lipscomb (1951)

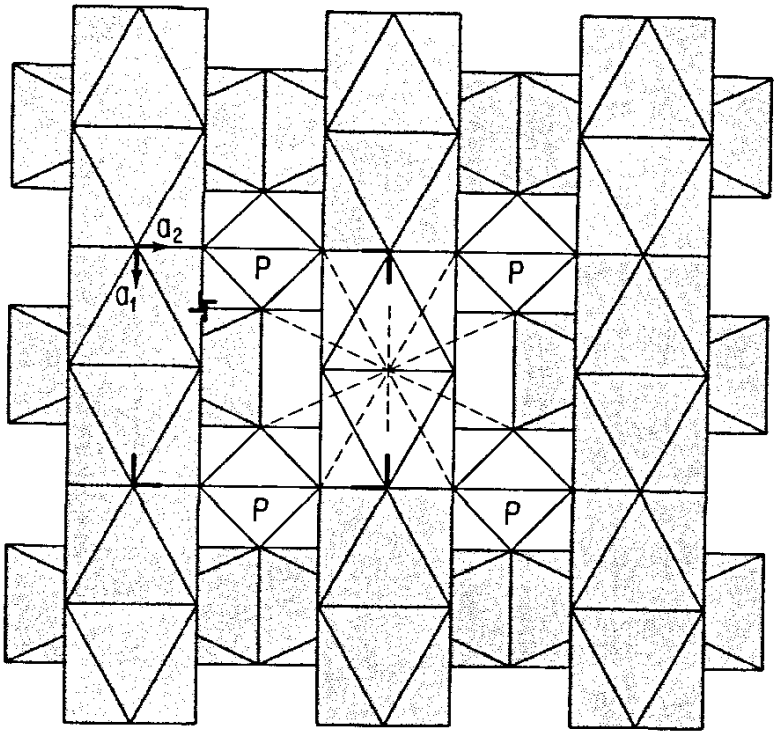

Fig. 1a. Idealization ($I4_1/amd$) of the lipscombite structure. Two stacks in succession of iron-oxygen face-sharing octahedra are stippled and PO_4 tetrahedra are denoted with the symbol P. The central ϕ (= Ca in scheelite) and its nearest neighbors are shown as dashed lines, their octahedra not stippled.

are compared with the scheelite structure type, see Table 4 and Table 5, to which these authors mentioned an affinity. Although they do not share the same point symmetry, the P → W and OH → Ca are isopunctal. The Fe → □ is very nearly isopunctal, the ordered vacancy residing on an invariant point in scheelite. The oxygen general positions deviate in the two structure types, with differences $\Delta = 0.73$ Å computed on the basis of the lipscombite cell. Thus, a rather remarkable case of partial antitypy arises, the compounds approximately related $Fe_8(OH)_4(PO_4)_4 \rightarrow \square_8Ca_4(WO_4)_4$.

The fundamental building block in 5 × 14 Å² structures

Moore (1970) outlined the crystal chemistry of a number of basic ferrosoferric phosphates. The species diversity of such compounds is probably large, but their deep green-black to deep orange colors and mimetic appearance render identification and distinction of such phases difficult. An underlying fragment, common to all known structures, was isolated, the so-called "*h*-cluster". It was noted that in many of the structures, "invariant" translations occur, a fiber axis direction of 5 Å and a remaining translation of 14 Å. This block of structure can be directly found in the lipscombite arrangement. It plays a central role in the known structures of lipscombite, scorzalite, dufrenite, rockbridgeite, beraunite, and several

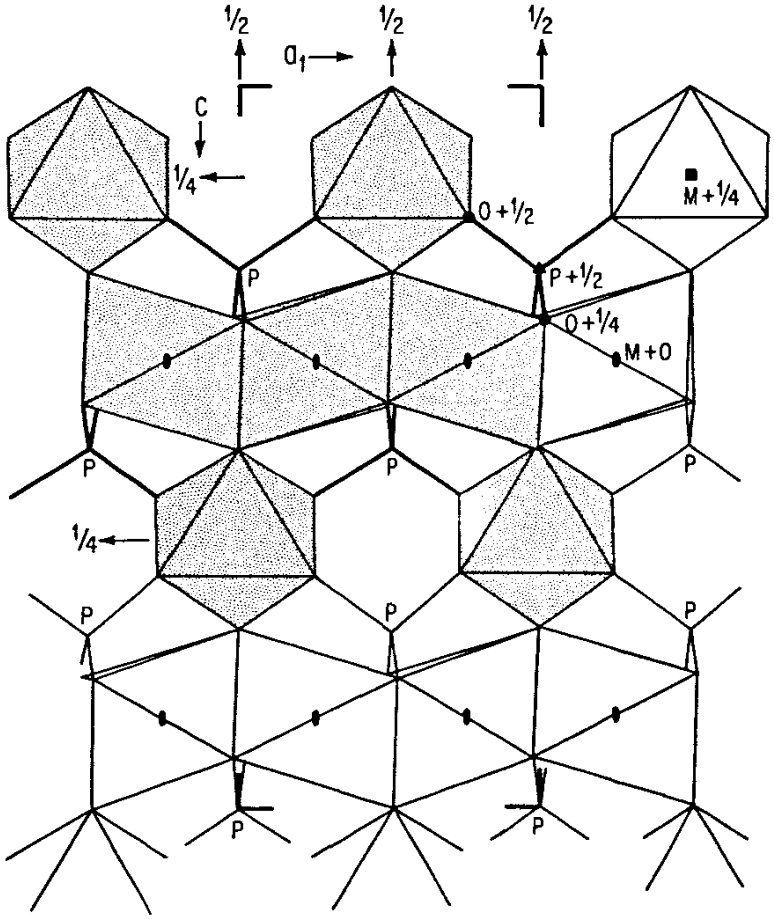

Fig. 1b. Idealization ($I4_1/amd$) of the lipscombite structure along [010] with the *h*-cluster octahedra stippled and tetrahedral P–O spokes drawn bold. Their centroids are denoted by P. The 5×14 Å^2 structures have $a' = a_1$ and $c' = -a_1 + c$. Some symmetry elements are drawn in.

other phases. More detailed re-investigation of all these curious 5 Å fiber axis structures would constitute a noble investigation by an energetic graduate student!

Figure 1a is an idealization of the lipscombite structure based on supergroup $I4_1/amd$, requiring only small movements of the Katz-Lipscomb atom centroids. It is an appealing design reminiscent of a rick of wood with logs in parallel orientation alternately rotated 90° by the 4_1-screw. Note the four central octahedra link to one central vertex of $\{T_d\}$ point symmetry. This is the ϕ ($\phi = OH^-, O^{2-}$) position of equipoint rank 4. It corresponds to the Ca position in partly antitypic scheelite, and potential nearest neighbor Ca–O bonds are dashed in Figure 1a. Bearing in mind that the difference in oxygen positions between lipscombite and scheelite is 0.73 Å, the coordination of ϕ (or Ca) is 8 + 4.

Figure 1b more closely represents the 5 Å fiber axis structures as they are portrayed. This is a projection of lipscombite along [010]. Here, the successive logs are oriented along and into the plane of the drawing. The

Table 4. Structure cells of beraunite and related phases.

	1 Beraunite	2 Beraunite	3 Beraunite	4 Lipscombite	5 MHSH	6 Scheelite
a	20.953(5)	20.760(3)	20.646(5)	5.37	5.242(1)	5.243(2)
b	5.171(1)	5.154(1)	5.129(7)	—	—	—
c	19.266(4)	19.248(2)	19.213(5)	12.81	12.995(3)	11.376(3)
$\beta(^\circ)$	93.34(2)	93.55(1)	93.62(7)	90	90	90
S.G.	*C*2/*c*	*C*2/*c*	*C*2/*c*	$I4_12_12$	$I4_1/amd$	$I4_1/a$
R	0.043, Iso.	0.034, Aniso.	0.068, Iso.	none	0.041, Aniso.	0.041, Aniso.

Notes: Rows include phases, cell parameters, space groups, *R*-index (if known), isotropic or anisotropic refinement. Columns refer to [1] present study; [2] Marzoni Fecia di Cossato et al. (1989); [3] Fanfani and Zanazzi (1967); [4] Katz and Lipscomb (1951); [5] Keefer et al. (1981); and [6] Kay, Frazer and Almodovar (1964).

Table 5. Eutaxies among lipscombite and related compounds.

Atom	1 Lipscombite ($I4_1/amd$)						Atom	2 Lipscombite ($I4_12_12$)					
	W	P	S	*x*	*y*	*z*		W	P	S	*x*	*y*	*z*
M	8*d*	1	2/*m*	1/2	1/4	1/8	Fe	8*f*	7/8	2	0.49	1/4	1/8
P	4*a*	1	$\bar{4}2m$	0	0	0	P	4*a*	1	222	0	0	0
OH	4*b*	1	$\bar{4}2m$	0	0	1/2	OH	4*b*	1	222	0	0	1/2
O	16*h*	1	*m*	0.24	0	0.07	O	16*g*	1	1	0.24	0.02	0.07
Atom	3 MHSH ($I4_1/amd$)						Atom	4 Scheelite ($I4_1/a$)					
	W	P	S	*x*	*y*	*z*		W	P	S	*x*	*y*	*z*
Mg	8*d*	2/3	2/*m*	1/2	1/4	1/8	□	8*d*	0	$\bar{1}$	1/2	1/4	1/8
S	4*a*	1	$\bar{4}2m$	0	0	0	W	4*a*	1	$\bar{4}$	0	0	0
O(2)	4*b*	1	$\bar{4}2m$	0	0	1/2	Ca	4*b*	1	$\bar{4}$	0	0	1/2
O(1)	16*h*	1	*m*	0.230	0	0.064	O	16*f*	1	1	0.241	0.151	0.086
H	16*h*	1/3	*m*	0.330	0	0.285							

Notes: Columns refer to atom, Wyckoff position (W), site population (P), point symmetry (S), atom coordinates (*x*,*y*,*z*). References are [1] holosymmetric ideal lipscombite; [2] Katz and Lipscomb (1951); [3] Keefer et al. (1981); and [4] Kay et al. (1964).

h-cluster is stippled and if isolated would have composition $M_7\phi_{18}(TO_4)_4$, ϕ = generalized anion, M = octahedron, T = tetrahedron. At the lower limit for known crystal structures, the face-sharing columns in the plane are ¾-occupied on average and those into the plane are ¼-occupied. The range is $M_8\phi_4(TO_4)_4$ to $M_4\square_4\phi_4(TO_4)_4$. The scorzalite group, for example, is in between with $M_6\square_2\phi_4(TO_4)_4$.

But most structures are monoclinic and approximate a slab which is 5×14 Å^2, while in lipscombite $a_1 = 5.37$, $c = 12.81$ Å. A cell transformation of Figure 1 b addresses this problem. Setting $a' = a_1$, $c' = -a_1 + c$, the $a' = 5.37$ and $c' = 13.89$ Å is obtained. This is evidently forced by ordered vacancies over the lipscombite aristotype which occur among these structures. The new cell now has $a' = 5.4$, $b' = 5.4$, $c' = 13.9$ Å, $\beta' = 113°$. There is a cascade in symmetry from $I4_1/amd \rightarrow P2/c$. This latter group is of considerable importance for it is included as a subgroup in the known structures of dufrenite, rockbridgeite, and beraunite; and is a subgroup of the proposed space groups for laubmannite, souzalite and kidwellite, all of unknown structure. Incidentally, the 5×14 Å^2 slab in the many structure types refers to the $b' \times c'$ plane.

The noteworthy feature is the persistence of the *h*-cluster among the known crystal structures. It is remarkable that the cluster appears in mineral crystals which have formed in a variety of paragenetic settings. Perhaps the lipscombite-scheelite partial antitypy is suggesting a similarity in vector sets derived from the Faltung of the structure factors, in particular the electrostatic model of structure stability (Ewald, 1973). Because structure types and their partial to complete antitypes necessarily have identical vector sets for their cross-terms, this notion is appealing as there exists — as yet — no means of predicting a structure type.

The MHSH structure

A quite remarkable relationship can be found between the lipscombite structure and that of $MgSO_4 \cdot \frac{1}{3}Mg(OH)_2 \cdot \frac{1}{3}H_2O$ (MHSH), space group $I4_1/amd$, $R = 0.041/160$ F_o reported by Keefer et al. (1981). Although the formula as expressed belies the fact that a direct relation exists with Figure 1 a (see also Table 4 and Table 5), rephrasing of the formulae sheds light on the relation. Write lipscombite as a series of two end-members:

$$(Fe^{2+}_{24/3})(OH)_4(PO_4)_4 - (Fe^{3+}_{16/3}\square_{8/3})(OH)_4(PO_4)_4 .$$

This is analogous to rephrasing MHSH as ($\times 4$):

$$(Mg^{2+}_{16/3}\square_{8/3})(OH)_4(SO_4)_4(H_{4/3}) .$$

The hypothetical holosymmetric Fe^{3+} lipscombite and MHSH are isostructural, with the exception of additional $^4/_3$H in the latter which is disordered ⅓-occupied hydrogen comprising the $OH_2 - OH^-$ join. These

disordered H atoms occur in the vacancies in the Mg sites. The relations among lipscombite-MHSH-scheelite make structure study a fascinating but humbling business and add further impetus to explore the structure stability as a vector set model of Ewald (1973).

Beraunite: it chemical crystallography

The big goal of this study is to provide satisfactory evidence of Fe-mixed valence ordering in a 5Å fiber axis crystal structure. Earlier accounts failed to provide unequivocal evidence because (1) the refinements were wanting in certain details, (2) the structures are rather complex, and (3) the crystals studied were oxidized members. We secured good data and proposed to test for ordering (if any) of Fe^{2+}/Fe^{3+} by bond distances, angles and electrostatic bond valences. Although we suspected that Fe^{2+} would preferentially order at the central Fe position of the face-sharing trimer, we could not find any compelling reason why this should be so. For example, Fe^{2+} may be more equitably distributed over the available Fe-sites in the crystal structure, over all trimeric sites only, or even at the octahedral termini of the trimer.

Figure 2 is a sketch of beraunite's crystal structure along the short fiber axis. The *h*-cluster is drawn in bold and stippled, and all atoms in the asymmetric unit are labelled. Proposed O—H···O bonds are shown as dashed lines. The (PO_4) tetrahedra are drawn as P—O spokes. Caution must be exercised, for nowhere in Figure 2 do tetrahedra share edges with octahedra but alternate in height along the *b*-direction. In effect, the *b*-axis is nearly the sum (~5.3 Å) of one octahedral (~2.8 Å) and one tetrahedral (~2.5 Å) edge.

The octahedrally coordinated cations M(2), M(3), and M(4) have (M—O) distance averages which range from 2.01 to 2.02 Å. The computed value for $^{[6]}Fe^{3+}$—$^{[3]}O^{2-}$ from Shannon and Prewitt (1969) = 2.01 Å. In fact, averages for MK, MOP and FZ in Table 3 range from 1.97—2.03 Å and the assumption that M(2), M(3), M(4) are Fe^{3+} sites is reasonable. The ⟨P(1)—O⟩ and ⟨P(2)—O⟩ distance averages are each 1.54 Å for all three entries in Table 3. The corresponding computed $^{[4]}P^{5+}$—$^{[2.5]}O^{2-}$ = 1.53 Å. Anomalous individual O(2) and O(3) bonds to M(4) and the terminal octahedra of the trimer will be discussed further under the bond valences.

The ⟨M(1)—O⟩ = 2.110 Å is a different matter. Calculations as above give $^{[6]}Fe^{2+}$—$^{[3]}O^{2-}$ = 2.13 Å and $^{[6]}Fe^{3+}$—$^{[3]}O^{2-}$ = 2.01 Å. This means that the M(1) site is about $^5/_6Fe^{2+} + {}^1/_6Fe^{3+}$ for the MK beraunite. The MOP results of ⟨M(1)—O⟩ = 2.045 Å gives about $¼Mn^{2+} + ¾Fe^{3+}$. The FZ average of 2.02 Å suggests a site with essentially Fe^{3+} occupancy. The results for the MOP sample are consistent with a significant content of Mn^{2+} solution into the M(1) site. They report a cation bond valence

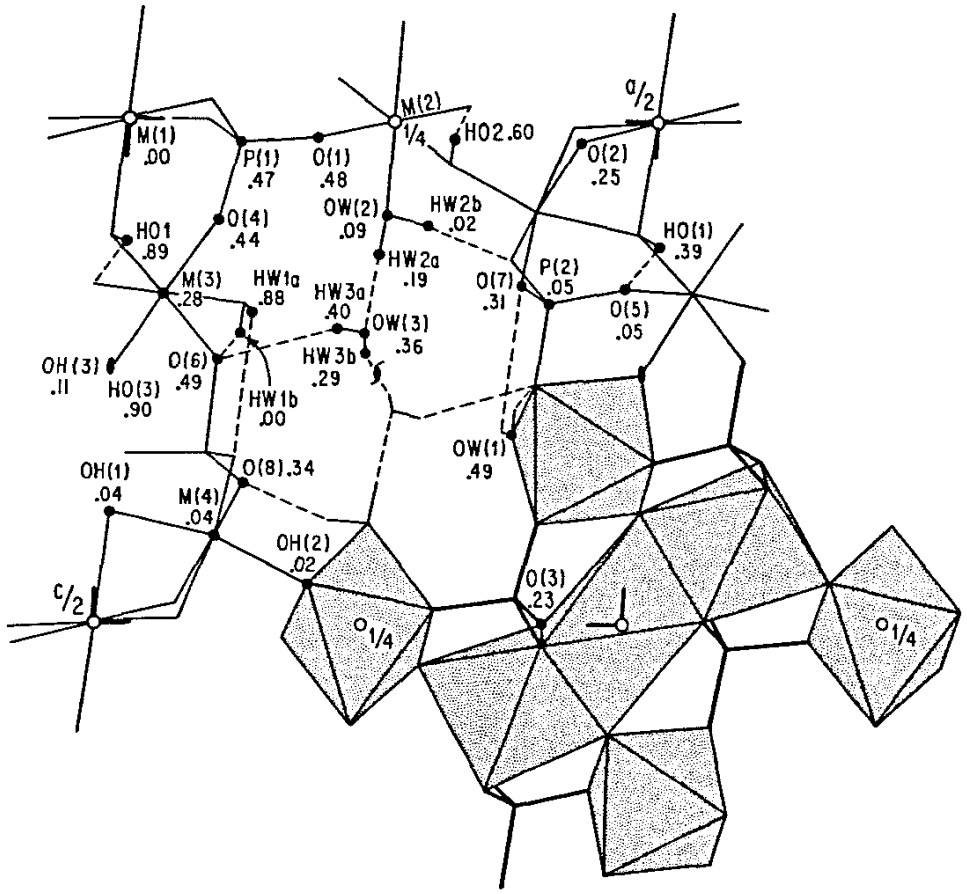

Fig. 2. The beraunite structure in the quarter cell along [010]. The *h*-cluster is drawn stippled and bold. The remainder are drawn as spokes. All atoms in the asymmetric unit are labelled. Proposed H-bonds from donor to acceptor are dashed in.

sum of +2.718 e.s.u. which is consistent with $\frac{1}{4}(2^+) + \frac{3}{4}(3^+) = +2.75$ e.s.u. for the $\langle M(1)-O\rangle$ bond distance average. They report 2.16 Mn^{2+} as cell contents, over twice our computed amount. We suspect that this excess Mn (as Mn^{2+}, or more likely Mn^{3+}) is distributed over some or all of the remaining M(2), M(3), M(4) sites.

Polyhedral distortions and bond valences

MOP proposed a bond valence sum for their manganoan beraunite from Mangualde, Portugal. We will confine our discussion to the octahedral face-sharing trimer which includes the cation sites M(1), M(3), M(4), and P(1); and the anion sites OH(1), O(2), and O(3).

To what extent does cation-cation repulsion occur across the shared faces of the M(4)–M(1)–M(4) trimer? To what extent is the system distorted from perfect octahedra and tetrahedra? The M(1)–M(4) distance through the OH(1)–O(2)–O(3) shared face can be calculated for the perfect model and compared with the computed distances for the three

structure refinements. The height, h, is the distance between two opposing faces in the octahedron (it corresponds to the layer separation in close-packing). From the tables of Shannon and Prewitt (1969), the $^{[6]}Fe^{3+} - ^{[3]}O^{2-}$ distance is $0.65 + 1.36 = 2.01$ Å. This corresponds to an edge $l = 2.01\sqrt{2} = 2.84$ Å, and $h = 2.84\sqrt{2}/\sqrt{3} = 2.32$ Å. For the structures, M(1)–M(4) = 2.874 (MK), 2.884 (MOP), and 2.870 (FZ) or an average of 2.88 Å, a lengthening of $\Delta = 0.56$ Å or $0.56/2.88 \times 100 = 19^{+}\%$ increase from the perfect model. Such an increase can be seen in Table 6, where O–O′ distances and O–M(4)–O′ angles associated with the shared face can be seen to consistently decrease with increasing Fe^{3+} content in the MK-MOP-FZ crystals.

A further check can be found in bond valence calculations based on Brown and Altermatt's (1985) procedure. The O(2) and O(3) oxide anions are each bonded to M(1), M(4), and P(1) and receive no H-bonds. The bond valence sums are $p_o = 2.00$, 1.98, and 2.00 electrostatic units (e.s.u.) for O(2) in the three crystals; and $p_o = 1.97$, 1.95, and 1.95 e.s.u. respectively for O(3) in these same crystals in the sequence MK-MOP-FZ. In other words, these oxides are nearly neutral, distinct from 2.08 e.s.u. for $Fe^{2+}Fe^{3+}P^{5+}$ in MK and 2.25 e.s.u. for $Fe^{3+}Fe^{3+}P^{5+}$ in MOP and FZ using the Pauling (1960) bond strength model. The bond valence model immediately explains M(4)–O(2), O(3) 2.08–2.09 in MK, and M(4)–O(2), O(3) 2.14–2.20 Å distances in MOP and FZ summarized in Table 6.

The remaining OH(1) ligand at the shared face presents a different problem. The oxide anion is bonded to M(1) + M(3) + M(4) + H(1). Bond valence calculation is hampered by the lack of precise determination of the H(1) centroid in all three studies. Small differences for the H(1) centroid would lead to large differences in bond valences. Because X-rays locate the bond pair centroid of O–H(1) but not the nucleus of H(1), Brown and Altermatt (1985) suggest, on empirical grounds, 0.95 Å for the O–H distance. This results in $p_o = 2.13$ (MK), 2.35 (MOP), and 2.40 (FZ) e.s.u., a progressive increase in bond valence sum with increasing Fe^{3+} content in these crystals. Loss of H(1) in these "overbonded" crystals would lead to extreme underbonding, with $p_o = 1.20$, 1.42, and 1.47 e.s.u. respectively, for $OH(1) = O^{2-}$, a flagrant contradiction in the longer than average bond distances noted in Table 6. We propose that achievement of local electrostatic neutrality proceeds according to the O–H(1) distance. For example, a neutral bond valence sum for FZ can be achieved by lengthening the distance to $d_{O-H(1)} = 1.09$ Å, an increase of +0.14 Å over 0.95 Å recommended by Brown and Altermatt (1985). This would imply that $d_{O-H(1)}$ progressively lengthens in the sequence of MK-MOP-FZ values. Such a model, which would have important implications in many structures with OH^{-} groups, should be testable by some independent spectroscopic technique. Unfortunately, without hydrogen loss, the system is not charge balanced.

Table 6. Beraunite selected bond distances and angles for face-trimer.

A	OH(1)–O(2)$^{(6)}$		O(2)$^{(6)}$–O(3)$^{(5)}$		OH(1)–O(3)$^{(5)}$	
MK	2.63	77.1	2.68	80.0	2.69	78.9
MOP	2.58	75.1	2.67	76.1	2.62	75.6
FZ	2.57	74.9	2.64	74.9	2.62	75.3
B	M(1)–OH(1)		M(4)–OH(1)		M(3)–OH(1)	σ
MK	2.12 (2.11)		2.13 (2.02)		2.03 (2.01)	$\pm$0.004 Å
MOP	2.02 (2.04)		2.08 (2.03)		2.01 (2.01)	$\pm$0.002 Å
FZ	2.01 (2.02)		2.08 (2.03)		1.99 (2.00)	$\pm$0.01 Å
C	M(4)–O(2)	M(4)–O(3)	M(4)–OH(1)	M(1)–O(2)	M(1)–O(3)	M(1)–OH(1)
MK	2.083	2.092	2.134	2.090	2.122	2.119
MOP	2.145	2.194	2.080	2.048	2.066	2.022
FZ	2.14	2.20	2.08	2.01	2.03	2.01

Notes: A Corresponds to shared octahedral face. Interatomic $\phi-\phi'$ distance (Å) and $\phi-M(4)-\phi'$ angles (°) are listed. Distances arranged according to increasing Fe^{3+}. **B** Corresponds to OH(1)–M bonds. Polyhedral average is given in parenthesis. Experimental errors (σ) are also given. **C** Corresponds to "anomalous" distances in trimer. All distances appear in Table 3.

Mention should be made of a disordered model. Clearly, in the absence of more detailed probes, in particular spectroscopic techniques, all arguments based only on three structure refinements of the trimeric face-sharing cluster remain speculative at best and vacuous at worst. The generally accepted homonuclear valence transfer-absorption mechanism $Fe^{2+} + Fe^{3+} \leftrightarrows Fe^{3+} + Fe^{2+}$ may well explain the colors deep green ($Fe^{2+}Fe^{3+}$) and orange ($Fe^{3+}Fe^{3+}$) common to the tribe of these "5 Å fiber axis structures". In beraunite, the disordered model

$$Fe(1)_4^{2+}OH(1)_8^{1-} \rightarrow Fe(1)_4^{3+}(OH_{1/2}O_{1/2})(1)_8^{1.5-}$$

(A) (B)

is especially appealing, and may equally well apply to all these related structures. The disordered model for cation coordination about OH(1) is an averaged model and involves M(1) + M(3) + M(4) + ½H(1). Computation of bond valence sums based on this model gives $p_o = 1.67$ (MK), 1.89 (MOP), and 1.94 (FZ) e.s.u. Recalling that the ordered model of MK gave $p_o = 2.13$ e.s.u., this suggests that the cluster in (A) applies for the MK crystal, but that (B) applies to MOP and FZ crystals. Such a scheme of disordered hydrogen is analogous to the MHSH phase of Keefer et al. (1981). For beraunite, the two end-members would be:

(A) $Fe^{2+}Fe_5^{3+}(OH)_5(H_2O)_4(PO_4)_4 \cdot 2H_2O$

and

(B) $Fe_6^{3+}O(OH)_4(H_2O)_4(PO_4)_4 \cdot 2H_2O$,

both with $Z = 4$.

But far more penetrating study, particularly focusing on H(1) and its behavior during Fe oxidation, will be required before the fundamental building block of the 5 Å structures is understood. Finally, the chemical relation above suggests a nomenclature which is wanting in the mineralogical literature: the reduced cluster (A) (deep green) would adopt the trivial mineral name and the oxidized cluster (B) (orange) would adopt the same name but with prefix "oxy-". Again, more penetrating spectroscopic study will be required before such nomenclature can be proposed.

Table 6 shows that the O—O′ edge distances and O—M—O′ angles associated with the shared face progressively decrease along the sequence, that is according to increasing Fe^{3+} content. This appears to be yet another strong indication of the cation-cation repulsion effect across the shared face. The Pauling (1960) third rule of cation-cation repulsion and polyhedral distortion has recently been discussed in some detail by Moore (1991). It was demonstrated that ionic radius sum and bond distance conservation, radius ratio, the first and second rules of Pauling; and the Brown (1981) bond valence rule fail for certain cation coordinations about a central anion

as a consequence of cation-cation repulsion. Such cation coordinations do not appear in beraunite, and the calculations offered here appear sensible.

Acknowledgements. This study was supported by the U.S. National Science Foundation, including NSF grant EAR-90-05742 toward the final synthesis and preparation of the manuscript. We thank Mr. Frank Leans of Philadelphia, PA (USA) for permission to submit his personally collected sample for chemical and structural study.

References

Brown, I. D.: The bond-valence method: an empirical approach to chemical bonding and structure. In: *Structure and Bonding in Crystals II* (M. O'Keeffe and A. Navrotsky, eds.). Academic Press, New York, 1–30 (1981).

Brown, I. D., Altermatt, D.: Bond-valence parameters obtained from a systematic analysis of the inorganic crystal structure database. Acta Crystallogr. **B41** (1985) 244–247.

Burnham, C. W.: Computation of absorption corrections, and the significance of the end effect. Am. Mineral. **51** (1966) 159–167.

Cromer, D. T., Liberman, D.: Relativistic calculation of anomalous scattering factors for X-rays. Los Alamos Sci. Lab., Univ. Cal. Rep. LA-4403, UC-34 (1970).

Cromer, D. T., Mann, J. B.: X-ray scattering factors computed from numerical Hartree-Fock wave-functions. Acta Crystallogr. **A24** (1968) 321–324.

Ewald, P. P.: Diffraction data and electrostatic energy of a crystal. Am. Crystallogr. Assoc. Program and Abstr. **1** (1973) 122.

Fanfani, L., Zanazzi, P. F.: The crystal structure of beraunite. Acta Crystallogr. **22** (1967) 173–181.

Frondel, C.: The dufrenite problem. Am. Mineral. **34** (1949) 513–540.

Katz, L., Lipscomb, W. N.: The crystal structure of iron lazulite, a synthetic mineral related to lazulite. Acta Crystallogr. **4** (1951) 345–348.

Kay, M. I., Frazer, B. C., Almodovar, I.: Neutron diffraction refinement of $CaWO_4$. J. Chem. Phys. **40** (1964) 504–506.

Keefer, K. D., Hochella Jr., M. F., De Jong, B. H. W. S.: The structure of magnesium hydroxide sulfate hydrate $MgSO_4 \cdot \frac{1}{3} Mg(OH)_2 \cdot \frac{1}{3} H_2O$. Acta Crystallogr. **B37** (1981) 1003–1006.

Marzoni Fecia di Cossato, Y., Orlandi, P., Pasero, M.: Manganese-bearing beraunite from Mangualde, Portugal: mineral data and structure refinement. Can. Mineral. **27** (1989) 441–446.

Moore, P. B.: Crystal chemistry of the basic iron phosphates. Am. Mineral. **55** (1970) 135–169.

Moore, P. B.: Betpakdalite unmasked, and a comment on bond valences. Submitted for publication (1991).

Palache, C., Berman, H., Frondel, C.: *The System of Mineralogy II*, 7th Ed., pp. 959–961. New York: John Wiley and Sons 1951.

Pauling, L.: *The Nature of the Chemical Bond*, 3rd Ed., pp. 543–562. Ithaca: Cornell University Press 1960.

Shannon, R. D., Prewitt, C. T.: Effective ionic radii in oxides and fluorides. Acta Crystallogr. **B25** (1969) 925–945.

Vencato, I., Mattievich, E., Mascarenhas, Y. P.: Crystal structure of synthetic lipscombite: a redetermination. Am. Mineral. **74** (1989) 456–460.